High Resolution Airborne Hyperspectral Data for Mapping of Ramin Distribution in Peat Swamp Forest

Mohd Azahari, F., Khali Aziz, H., Hamdan, O.

High Resolution Airborne Hyperspectral Data for Mapping of Ramin Distribution in Peat Swamp Forest

High Resolution Airborne Hyperspectral Data for Mapping of Ramin Distribution in Peat Swamp Forest

Mohd Azahari, F., Khali Aziz, H., & Hamdan, O.

2011

First Printing 2011

All enquiries should be forwarded to:

Director-General
Forest Research Institute Malaysia (FRIM)
52109 Kepong, Selangor Darul Ehsan, Malaysia
No. Tel: 603-62797000
Fax: 603 62731314
http://frim.gov.my

Perpustakaan Negara Malaysia Cataloguing-in-Publication Data

High Resolution Airborne Hyperspectral Data for Mapping of Ramin Distribution in Peat Swamp Forest / editors Mohd Azahari, F., Khali Aziz, H., and Hamdan, O.

I. Institut Penyelidikan Perhutanan Malaysia
II. Title

Set in Cambria/11 point

Printed in Malaysia by Gemilang Press Sdn. Bhd., Sungai Buloh

CONTENTS

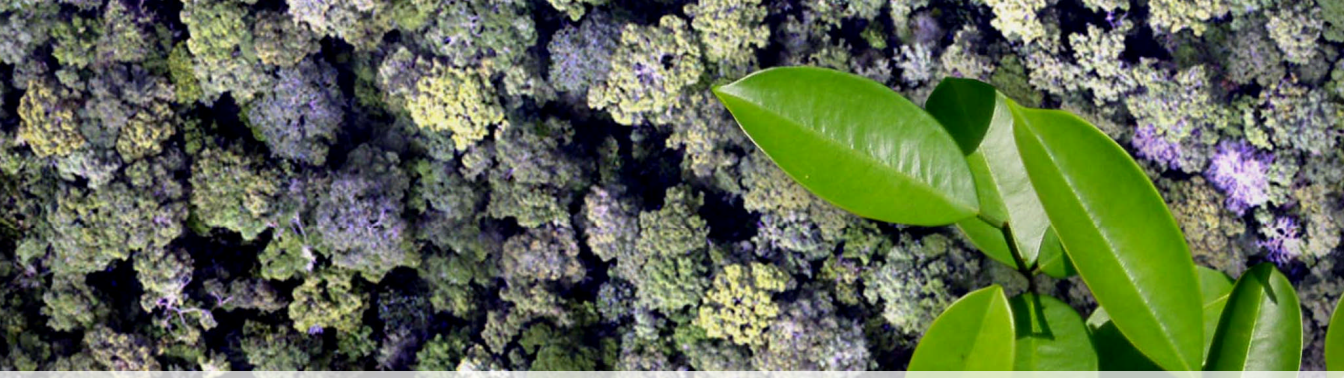

List of Figures

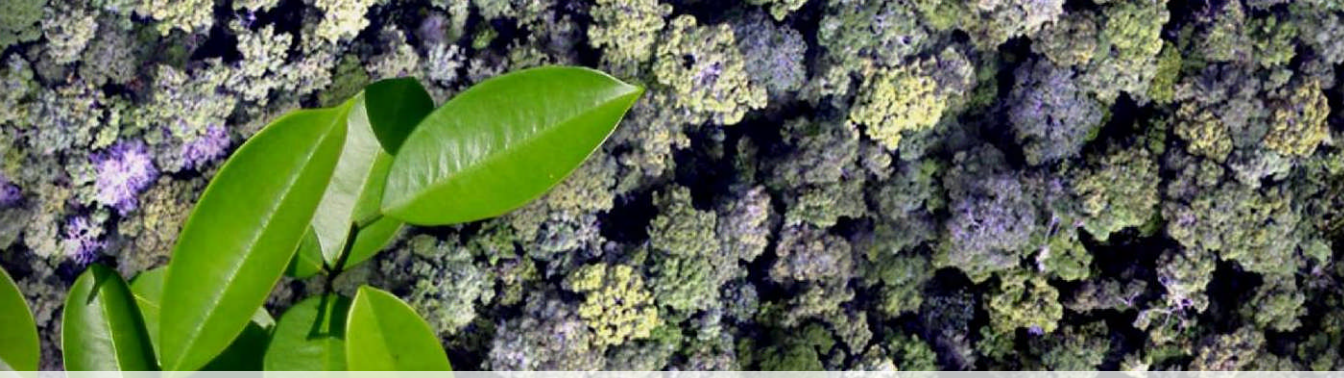

List of Tables

Preface

Peat swamp forest (PSF) is the largest of the wetland forests in Malaysia and consists of some of Malaysia's endangered tree species such as *Gonystylus bancanus.* This species has been listed in Appendix II of the Convention on International Trade in Endangered Species of Wild Fauna and Flora (CITES) and as such needs better management and control. Among others, spatial distribution information on the species in the natural environments need to be identified and mapped. The developments of airborne hyperspectral remote sensing have provided new opportunities for mapping this tree species at a landscape scale. A recently concluded study in Malaysia's tropical peat swamp forest exhibited a promising use of airborne hyperspectral data for mapping *G. bancanus* distribution. The study was conducted in Pekan Forest Reserve, Pahang, using HySpex VNIR-1600 airborne hyperspectral data with the spatial resolution of 0.5 meter and spectral range of 400 nm to 1000 nm. It was found that the HySpex airborne hyperspectral data have good capability to discriminate individual canopy layer tree species in mixed peat swamp forest. The distribution of *G. bancanus* in the natural peat swamp forest could be mapped with an accuracy of 86%. It is anticipated that with the availability of accurate information on the *G. bancanus* population derived from airborne hyperspectral data, better management of the species for both conservation and sustainable use can be undertaken.

Mohd Azahari Faidi
Khali Aziz Hamzah
Hamdan Omar

Acknowledgements

This work was made possible by a grant from the International Tropical Timber Organization (ITTO) under its collaborative programme with the Convention on International Trade in Endangered Species of Wild Fauna and Flora (CITES) to build capacity for implementing timber listings. Donors to this collaborative programme include the European Union (EU) (primary donor), the USA, Japan, Norway, New Zealand and Switzerland.

We would like to extend our thanks to the Ministry of Natural Resources and Environment (NRE) for their full support throughout the project. Our special thanks also go to all the collaborating agency, namely the Forestry Department Peninsular Malaysia (FDPM) includes the Headquarters and the State Forestry Department of Pahang. Without which their full support, the collection of data in the peat swamp forest would not have been possible.

Last but not least, our gratitude also goes to Dato' Dr Abd. Latif Mohmod, the Director General of FRIM for giving us his support and encouragement during the preparation of this manuscript.

Project Identification

Project number: Activity 3
Host Government: The Government of Malaysia (GOM)
Name of the Executing Agency and Project Coordinator: Ministry of Natural Resources and Environment (NRE)
Starting date of the Project: September 2008
Duration of the Project (month): 24 months

CHAPTER 1
INTRODUCTION

With the advancement of new technology in remote sensing such as high resolution and multi-spectral images, discrimination of forest species using this technology is emerging. Several efforts have been initiated and demonstrated on the potential of using the hyperspectral images for tropical rainforest tree species identification while others have used aerial photographs and high spatial resolution multispectral data such as IKONOS (1 m and 4 m) and Quickbird (0.7 m and 2.8 m) for the same purposes. Hyperspectral imagery is a significant technology used in remote sensing and plays an important role in the success of image classification because it provides valuable spectral information on the objects of interest captured in the imagery.

A study to test the applicability of airborne hyperspectral remote sensing data for peat swamp forest tree species mapping was carried out in a tropical peat swamp forest of Malaysia. This study was undertaken to discriminate individual *G. bancanus* in the natural environment with intention of mapping its population distribution. Further information on *G. bancanus* was given in detail by Khali et al. (2010) in a book entitled *"Gonystylus bancanus – Jewel of the Peat Swamp Forest"*. Based on the peat swamp forest profile (Figure 1), *G. bancanus* can be classified as a canopy layer tree (Khali et al. 2009). Thus it gives an advantage to delineate *G. bancanus* using airborne hyperspectral data.

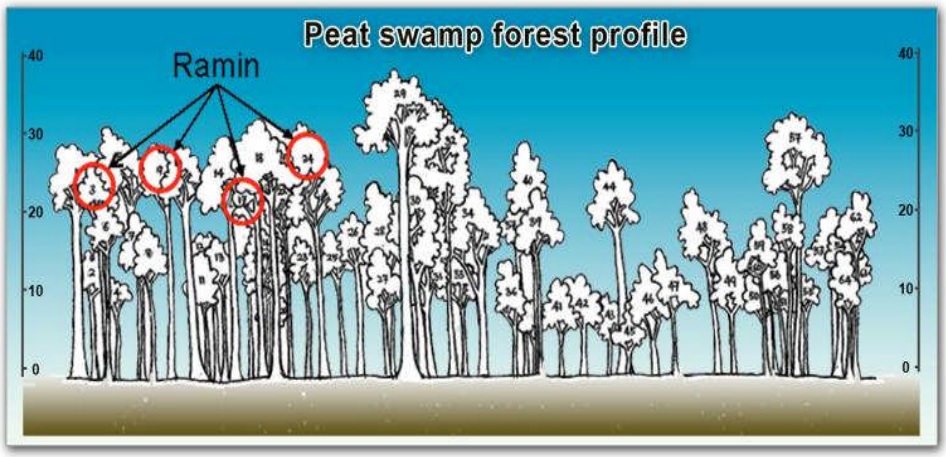

Figure 1 Peat swamp forest profile showing *G. bancanus* (ramin) as a canopy layer tree

CHAPTER 2
HYPERSPECTRAL IMAGING

Hyperspectral Remote Sensing

The importance of remote sensing in providing information for forest management has been widely recognized. It is one of the ways to acquire repetitive forest biophysical data for large geographic area at reasonable cost, accuracy and effort. In forestry, the use of remote sensing is generally based on the assumption that spectral response of forest canopy is highly correlated with the forest parameters such as tree density, height and diameter breast height. Hence, those forest variables can be indirectly measured from the spectral response of the forest canopy (Danson 1995).

Multi-spectral remote sensing images have been used in forest classification for many years. The multi-spectral sensors include the Advanced Spaceborne Thermal Emission and Reflection Radiometer (ASTER), the Landsat Thematic Mapper (TM), and Satellite Pour l'Observation de la Terre 5 (SPOT 5). However, multi-spectral images have poor capability of discriminating forest species precisely. With the development of hyperspectral remote sensing system (Figure 2), it has been used to improve the classification accuracy. Studies have shown that hyperspectral remote sensing is a powerful diagnostic tool for agriculture, environment and ecology, aquaculture, forestry, geosciences, and other disciplines of studies (Buckingham et al. 2002).

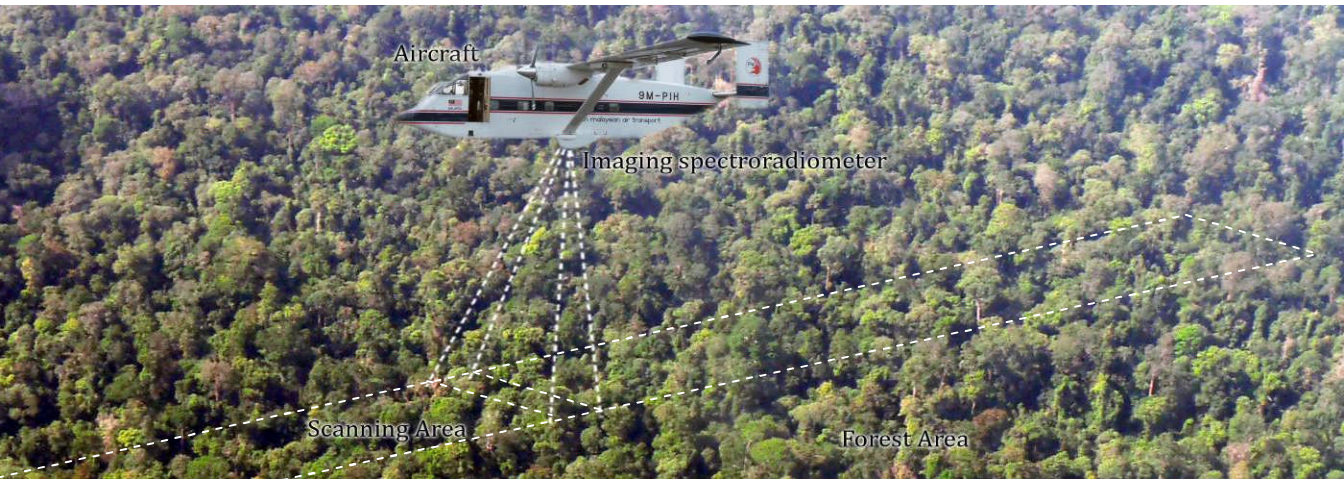

Figure 2 Airborne Hyperspectral data acquisition technique

The naming of hyperspectral images is suitable from the perspective of this definition when one considers their attributes in relation to a traditional colour image. A standard computer representation of an image simply contains red, green, and blue components that can be combined to create a color image. In contrast, hyperspectral images can be thought of as a set of many images that represent measurements of the reflectance of light at closely spaced wavelengths, often including data outside of the visible spectrum. Hyperspectral sensors measure energy in narrower and more numerous bands than multispectral sensors. In hyperspectral images, each spatial element has a continuous spectrum that is used to analyse the features in the images (Figure 3).

Hyperspectral images can contain as many as 200 (or more) contiguous spectral bands. The numerous narrow bands of hyperspectral sensors provide a continuous spectral measurement across the entire electromagnetic spectrum and therefore are more sensitive to subtle variations in reflected energy. Images produced from hyperspectral sensors contain much more data than images from multispectral sensors and have a greater potential to detect differences among land and water features. For example, multispectral imagery can be used to map forested areas, while hyperspectral imagery can be used to map tree species within the forest.

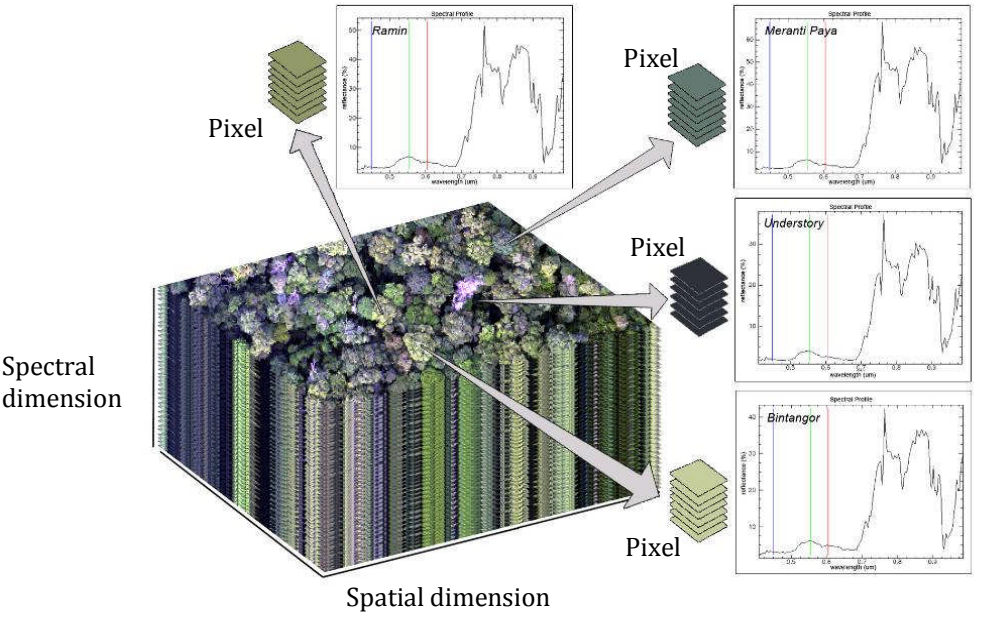

Figure 3 Hyperspectral data cube

Vegetation Spectral Signature

Features on the Earth reflect, absorb, transmit and emit electromagnetic energy from the sun. Hyperspectral imaging system has been developed to measure all types of electromagnetic energy as it interacts with objects. A measurement of energy commonly used in remote sensing forestry application is reflected energy such as visible light and near infrared that come from forest canopy surfaces. The amount of energy reflected from these surfaces is usually expressed as a percentage of the amount of energy striking the objects. Across any range of wavelengths, the percent reflectance values for peat swamp forest features can be plotted and compared. Such plots are called "spectral response curves" or "spectral signatures".

Figure 4 shows the spectral curves of five selected peat swamp forest features namely; water, understory vegetation, bintangor (*Calophyllum ferrugineum*), meranti paya (*Shorea platycarpa)* and ramin (*Gonystylus bancanus*). This demonstrates that the selected spectra exhibit minimal variability in terms of magnitude in the visible wavelengths and a large rise in variability as the wavelengths increase towards the near-infrared wavelengths, especially the bands between 0.75 and 0.850 µm. A distinct separation between ramin and the other features is shown at 0.55 µm.

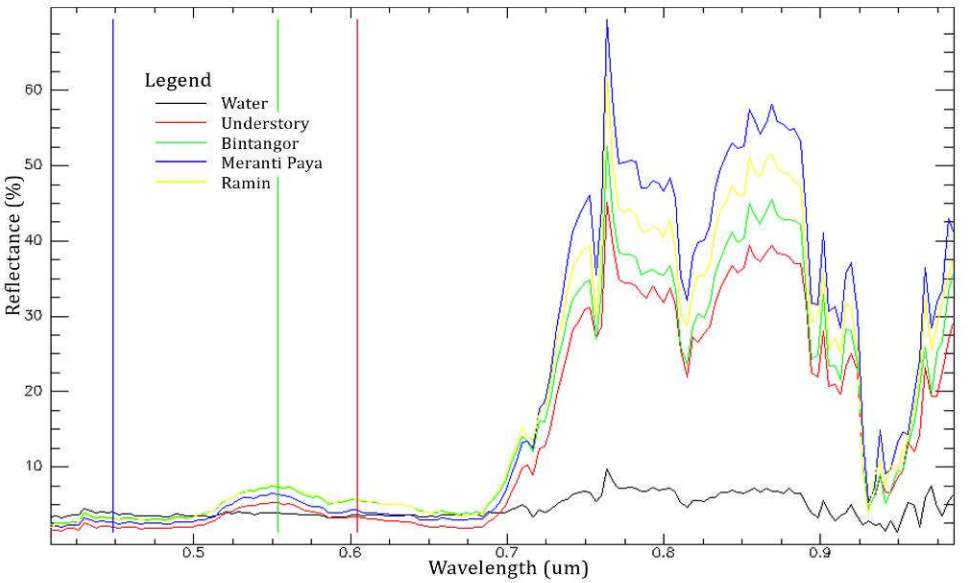

Figure 4 Spectral signatures of selected peat swamp forest features

Reflectance is 100% if all of the light striking objects, bounces off and is detected by the sensor. If none of the light returns from the surface, reflectance is said to be 0%. Generally, the reflectance value of forest species is different between each other. Differences among spectral signatures are used to help classify remotely sensed images into classes of landscape features since the spectral signatures of like features have similar shapes. The more detailed the spectral information is recorded by a sensor, the more information that can be extracted from the spectral signatures. Hyperspectral sensors have much more detailed signatures than multispectral sensors and thus provide the ability to detect more slight differences in terrestrial features.

Hyperspectral image has great potential to be used to extract information in a fairly uniform landscape such as peat swamp forest. One would expect that the increment in the number of bands in hyperspectral image will result in an increase in the classification accuracy in comparison with multispectral sensors. On the other hand, application of hyperspectral images also brings some problems. High-dimensional datasets of hyperspectral image prominantly contains huge data volume and the narrow band tends to be strongly related with the adjacent ones, leading to mixed and useless signals. However, with the right approach and processing and analysis procedures, variations within peat swamp can be discriminated and classified accordingly in the hyperspectral image.

CHAPTER 3
APPLIED METHODOLOGIES

Introduction

To identify and locate ramin trees in a highly mixed heterogeneous rainforest is a challenging task. The most promising tool or method to overcome the problem is by applying airborne remote sensing hyperspectral technique. The introduction of hyperspectral technology, which produces much more complex imagery, provides the abilities to distinguish individual tree species in mixed forest ecosystem. However, it insists on more complex and sophisticated data analysis procedures before the full potential use of the hyperspectral data can be achieved. The flowchart of the general methodology for ramin mapping using airborne hyperspectral technology is presented in Figure 5.

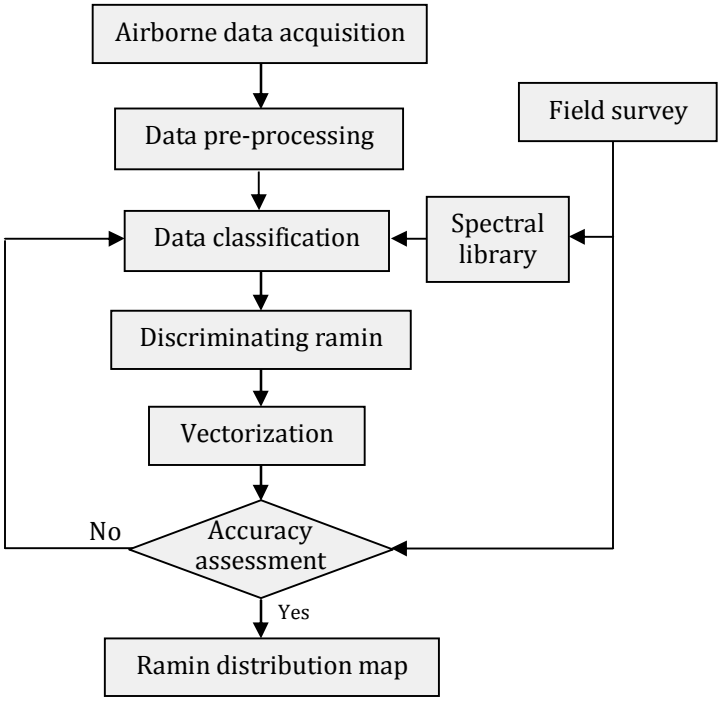

Figure 5 Flowchart of general methodology for ramin mapping using airborne hyperspectral data

Project Area

The study area, Pekan Forest Reserve is located at 593637.380 E and 379195.379 N in the South-East Pahang Peat Swamp Forest, Pahang (Figure 6). The project area experiences a relatively dry period lasting about eight months from February to September, followed by four months of heavy rain between October and January, the peaks being in December and January (Abdul Rahim, et al. 2007). The management of the forest reserve is undertaken by the state Forestry Department (FD) and complies with the *Malaysian Criteria and Indicators for Forest Management Certification* [MC & I (2002)] requirements.

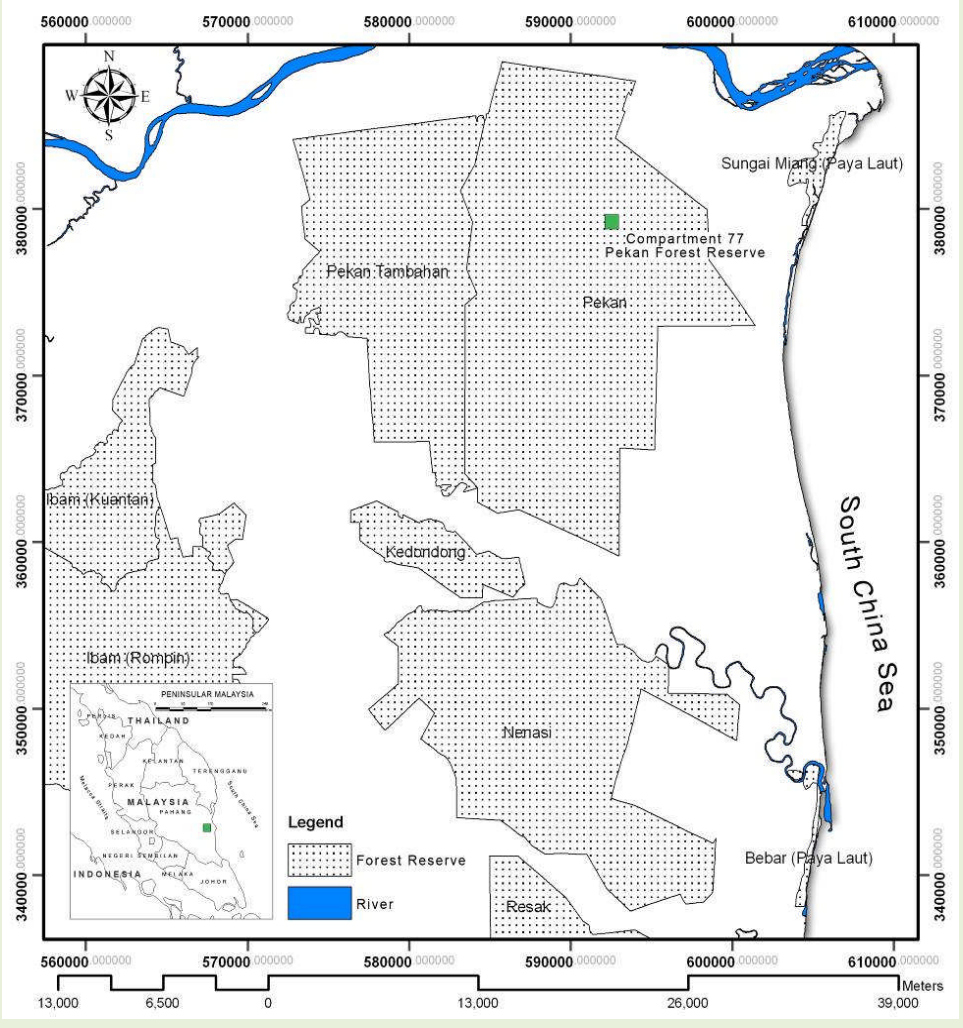

Figure 6 Location of the study area

The Pekan Forest Reserve has 106 species of trees belonging to 72 genera and 32 families (Abdul Rahim et al. 2007). The dominant families in terms of relative numbers in the reserve are *Guttiferae* (bintangor), *Myrtaceae* (kelat), *Myristicaceae* (penarahan) and *Burseraceaee* (kedondong). Other important families are *Leguminonasae* (kempas), *Thymelaeaceace* (ramin), *Ebeneceace* (kayu arang) and *Annonaceace* (mempisang). In term of basal area, *Calophyllum ferrugineum* (Guttiferae) records the highest, followed by *Gonystylus bancanus*, *Tetramerista glabra*, *Koompassia malaccensis* and *Durio carinatus*.

Test Plot Area

The test plot area of 6.25 ha was selected from the total 200 ha of project area (Compartment 77, Pekan Forest Reserve). This test plot consists of about 53 test blocks (30 m x 30 m) (Figure 7). Data collections through field inventory and data verification through spectral signature sampling were carried out within this test plot.

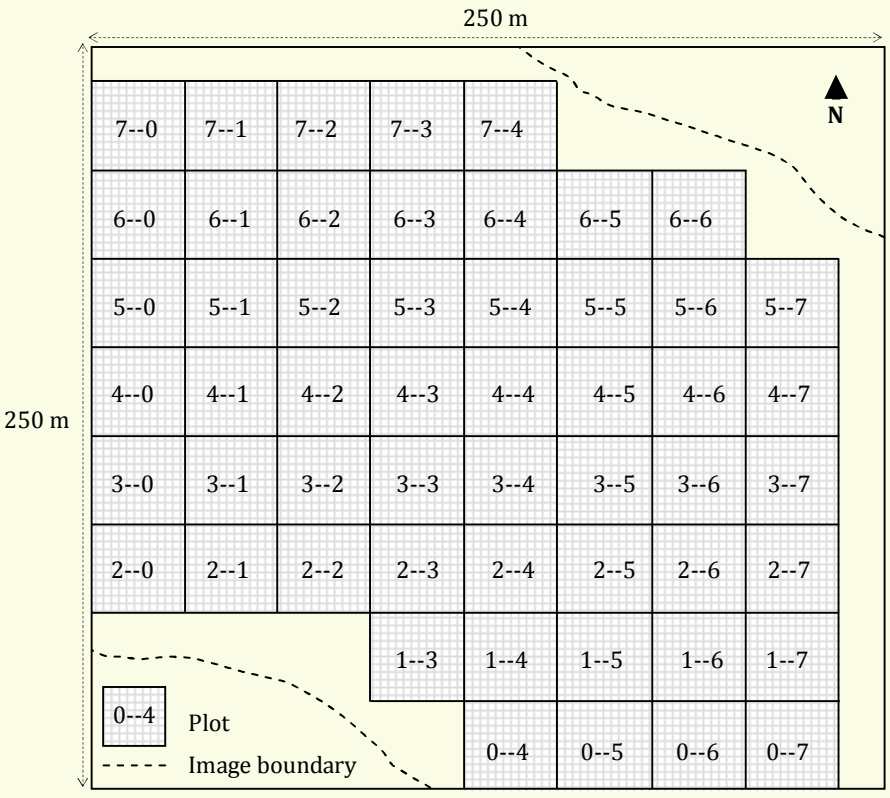

Figure 7 Test plot area

HySpex VNIR 1600 Hyperspectral Data Acquisition

The HySpex VNIR-1600 sensor (Figure 8) is an airborne sensor produced and operated by the company Norsk Electro Optic (NEO). The HySpex camera images the scene line by line using a so-called "pushbroom" scanning mode. In the VNIR mode, HySpex acquires radiance in 160 bands, ranging from 400 nm to 1000 nm, each with a bandwidth of 3.7 nm (Table 1). The hyperspectral data that was acquired on 15 January 2010 along the test plot lines in the project area was used as the primary input for this study.

Table 1 HySpex VNIR 1600 characteristic

Specifications	Characteristic
Module	VNIR-1600
Sensor Type	Pushbroom Si CCD 1600
Spectral range	0.4 – 1 µm
Spatial pixels	1600
FOV across track	17°
Pixel FOV across track/along track	~0.185 mrad / 0.37 mrad
Spectral sampling	3.7 nm
Spectral bands	160
Data format	12 bit
Frame frequency	120 fts

Figure 8 Airborne HySpex VNIR 1600 systems installations

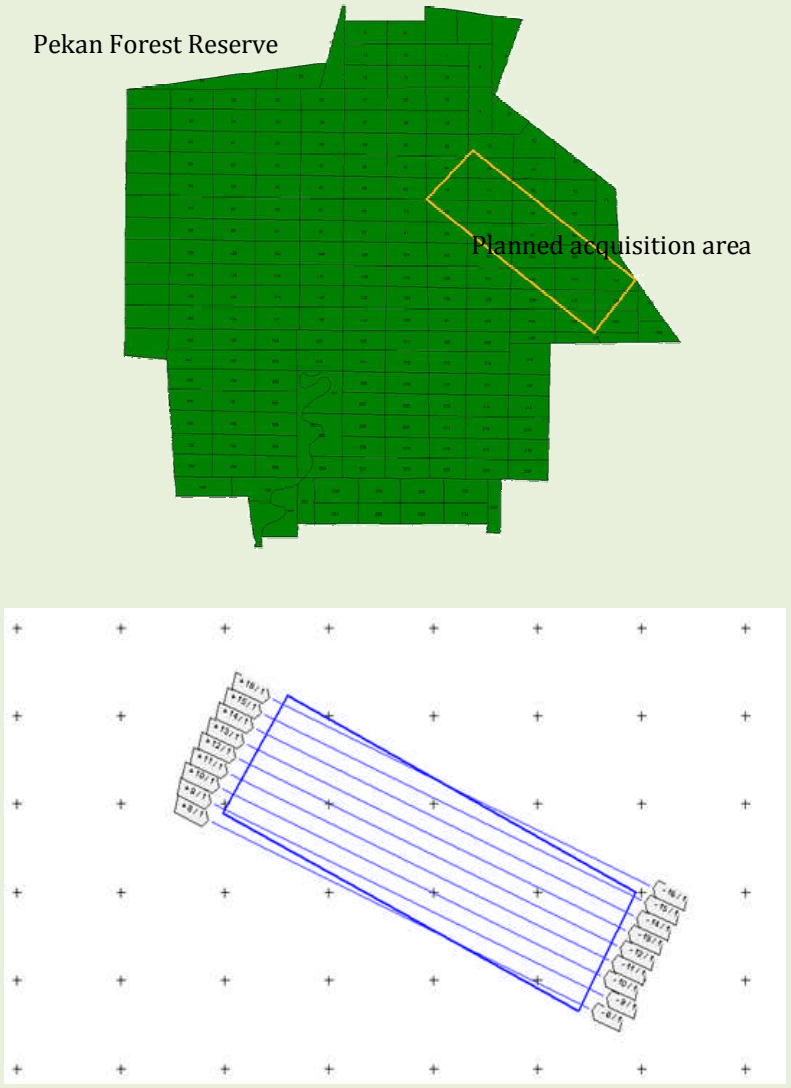

Figure 9 Planned flight path

By scanning over the scene, the HySpex camera collects slices from adjacent lines that have been planned (Figure 9), forming a hyperspectral image or "cube", with two spatial dimensions and one spectral dimension. The HySpex sensor is also capable of recording in the SWIR (Short Wave InfraRed) mode, but this mode was not available for this project. The SWIR mode ranges from 1000 to 1700 nm. The pixel size of the image captured was 0.5 meter.

Acquisition of hyperspectral data which is the core activity in this study was done by a team of experts engaged by the project. The chronology of data acquisition activity is summarized in Figure 10 below.

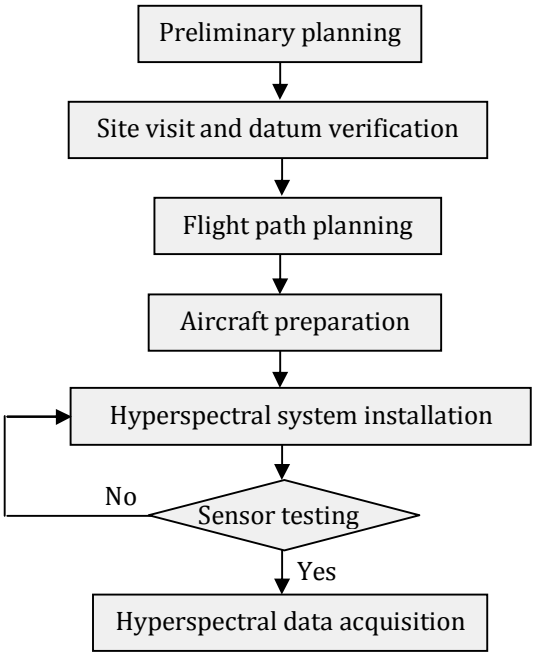

Figure 10 Chronology of hyperspectral data acquisition

On-Site Data Collection

There are at least three aspects of airborne hyperspectral imagery data processing that often require on-site data collection. First is the validation of the spatial integrity of the imagery through the datum position (x,y) verification, second is the spectral signature measurement using Spectroradiometer equipment for creation of a custom spectral library and the third is the tree inventory activity for sampling and output verification.

Datum Verification

A Differential Global Positioning System (DGPS) monument in Compartment 77, Pekan Forest Reserve, established by Forest Research Institute Malaysia (FRIM), was used as reference point for airborne track planning during the hyperspectral data acquisition (Table 2). This monument was also used for

the determination of ramin tree positions in the field during the field inventory. The verification survey was done within the Position Dilution of Precision (PDOP) value of 3 – 12. PDOP is a measure of the quality of the GPS data being received from the satellites. DOP is a mathematical representation for the quality of the GPS position. The main factors affecting DOP are the number of tracking satellites and where these satellites are positioned in the sky.

Table 2 FRIM DGPS monument position

Point	East (x)	North (y)	Height (z)
FRIM DGPS Monument	593637.380	379195.379	7.836

Spectral Signature Measurement

In attempting to study the spectral signature of ramin, it is very crucial to assess and compare its spectral reflections between laboratory and on-site measurements. The process will give better understanding of the effects of environment on the ramin spectral reflectance patterns. In this project, a handheld GER 1500 Spectroradiometer (Table 3 and Figure 11) device acquired by FRIM on September 2009 was used to measure the spectral signature of ramin leaf.

The ideal way to measure and collect the spectral signature on the ground using handheld spectroradiometer is to conduct the measurements and collection at the same time as the airborne hyperspectral sensor is flown. However, in most cases this is difficult to, do and as such collection at approximately the same atmospheric conditions as the hyperspectral data collection on a different day is sufficient.

Table 3 Specifications for GER 1500 Spectroradiometer

Detail	Specifications
Spectral Range	350 nm to 1050 nm
Internal Memory	400 scans
Band	512
Bandwidth Sampling	1.5 nm
Scan Time	5 ms and up (selectable)
FOV	4 degree
Weight	2 kg
Battery Type	6 Volt NiMH

Figure 11 GER 1500 Spectroradiometer

Tree Inventory

Field inventory to collect ramin tree information was carried out in the test site (Figure 12).

Figure 12 Field survey activities

Plot blocks, each with an area of 30 m x 30 m were established in the test area and within this block parameters including the x,y location, diameter breast height (dbh), total height, 1st branch height and crown width of all ramin trees with dbh above 20 cm were measured and recorded. The collected data were kept in a GIS database for future reference. Besides ramin, a bintangor species (*Calophyllum ferrugineum*) in the test plot was also enumerated and recorded as a reference to the ramin tree distribution.

Data Preprocessing

Two image pre-processing routines, namely geometric and radiometric correction were performed on the hyperspectral data. The data were geometrically corrected and rectified and conformed to the Malaysian Rectified Skew Orthomorphic (RSO) projection system. The hyperspectral data were not mosaic in order to keep the authenticity of each individual hyperspectral stripe. With 160 different channels of hyperspectral data, it was necessary to do some data reduction before the analyses.

The reduction of the dimensionality of the hyperspectral data is based on a forward MNF (Minimum Noise Fraction) rotation. The MNF rotation transforms are normally used to determine the inherent dimensionality of image data, to segregate noise in the data, and to reduce the computational requirements for subsequent processing. The reduction of the channels was based on a threshold of 2 and reduced the 160 bands to 23 bands with an acceptable noise ratio and variability.

Data Classification

Spectral characteristic of vegetation from hyperspectral images are closely related to the physical properties of tree leaves. Each vegetation species will give a different spectral response to electromagnetic radiation in terms of reflectance and absorption in visible near infrared (VNIR) and short wave infrared (SWIR) regions. In this study, the Spectral Angle Mapper (SAM) technique was used to classify ramin in the study area. The SAM technique is a physically based spectral classification that uses an n-dimensional angle to match pixels to reference spectral. This is shown in Figure 13, where a two-band "spectrum" will lie somewhere along a line passing through the origin of a two-dimensional space.

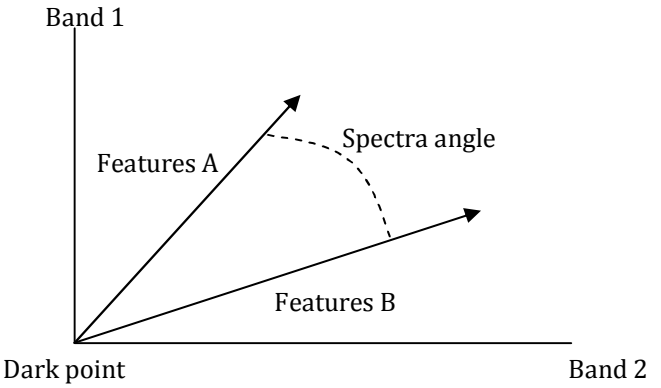

Figure 13 Two-dimensional spectral angle

The SAM technique is based on the idea that an observed reflectance spectrum can be considered as a vector in a multi-dimensional space, where the number of dimensions equals the number of spectral bands (Shafri et al. 2007). SAM compares the angle between the end member spectrum vector and each pixel vector in n-dimensional space. Smaller angles represent closer matches to the reference spectral. Pixels further away than the specified maximum angle threshold in radians are not classified.

In this study, identified pixels that represent patterns of individual ramin species were selected with the help of the ramin position information from field survey activity. In this process, knowledge of the tree species classes is required before the classification process can be performed. The selected ramin tree that has been identified will be use as a sample point to generate ramin spectral signature in the SAM classification technique. Based on the spectral signature pattern, the computer system will be instructed to identify and classify pixels with similar characteristics. The output from this process is a ramin distribution map in raster format.

Map Production

The raster format map generated from the above process is further converted to vector format. In order to have the vector polygons available for use in a GIS, the vectors were exported to the Shapefile format polygon region coverage. To ensure the classification accuracy of the ramin distribution information derived from the hyperspectral data, an accuracy assessment of the map is carried out. Accuracy can be defined as a degree of correspondence between observation and reality (true data). Usually, the

assumed true data are derived from ground survey data. However, it is not practical to undertake hundred percent ground truth survey or to test every pixel of the classified image. Therefore, a set of reference points is usually used. In this project, the reference point selected is based on reference information or ground data using a systematic sampling method. Error matrices will be produced from the classification results based on the individual ramin tree position.

CHAPTER 4
RESULTS AND ANALYSIS

Introduction

The airborne HySpex VNIR 1600 hyperspectral data that were acquired on 15 January 2010 along the test plot lines in the project area were used as the primary input for this study. It is important to understand the data acquisition process in order to process the hyperspectral data properly before useful information is extracted. In total about 20 scenes of hyperspectral images had been captured to cover the 2000 ha of the study area. However, only one scene had been processed to discriminate G. bancanus in the study area. Figure 14 shows the subset of the hyperspectral data that were analyzed in this study.

Hyperspectral Band combination

With 160 different channels of hyperspectral imagery, it is necessary to get the best band combination to enhance the imagery. For the HySpex VNIR 1600 airborne hyperspectral data, the best "natural" colour (true colour) representation is in the form of bands 55, 41 and 12 (R,G,B) combination. Visual comparison of combination bands 55, 41, and 12 (true colour) with the pseudo colour combination of bands 159, 43, 13 shows that the pseudo colour combination discriminates more features. Hence, in this project, the pseudo-colour combination was used in preparing the individual canopy tree sample for classification of the hyperspectral data. Figure 15 shows the difference between natural colour and pseudo-colour band combinations.

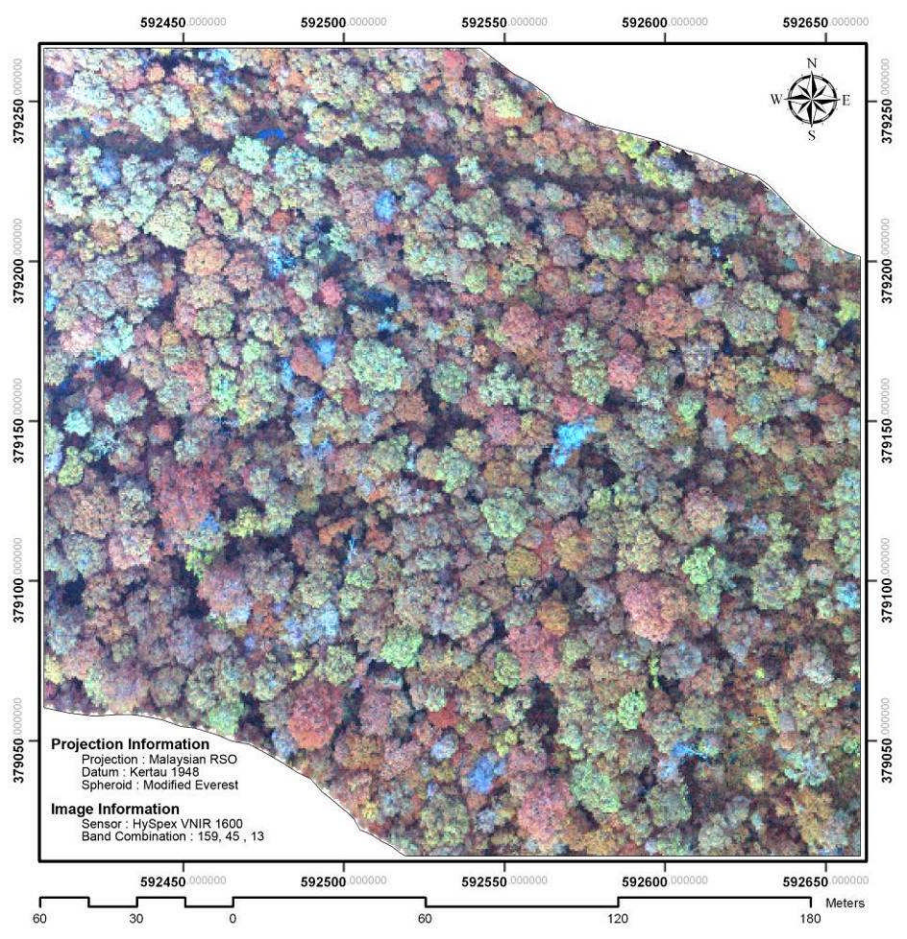

Figure 14 Selection of hyperspectral data in the study area

(a)

(b)

Figure 15 Hyperspectral band combination: (a) Natural colour 55, 41, 12 (b) Pseudo-colour 159, 38, 13

Spectroradiometer for Spectral Signature Measurement

Spectral signatures of ramin and bintangor in the study area were measured using spectroradiometer. This is necessary in order to determine the spectral reflectance values of both species as a guide prior to classification of the hyperspectral image.

Figure 16 Spectroradiometer data measurement activities

The spectral reflectance data of ramin and bintangor that had been measured in the field survey (Figure 16) were plotted as spectral curves. These spectral curves were analysed and assessed in order to determine tree species separability. Figure 17 below shows the different spectral signature curves for ramin and bintangor.

Table 4 Statistics of spectral signature measurement

Statistic	Ramin (%)	Bintangor (%)
Minimum	2.2	6.2
Maximum	57.9	59.6
Mean	26.9	31.7

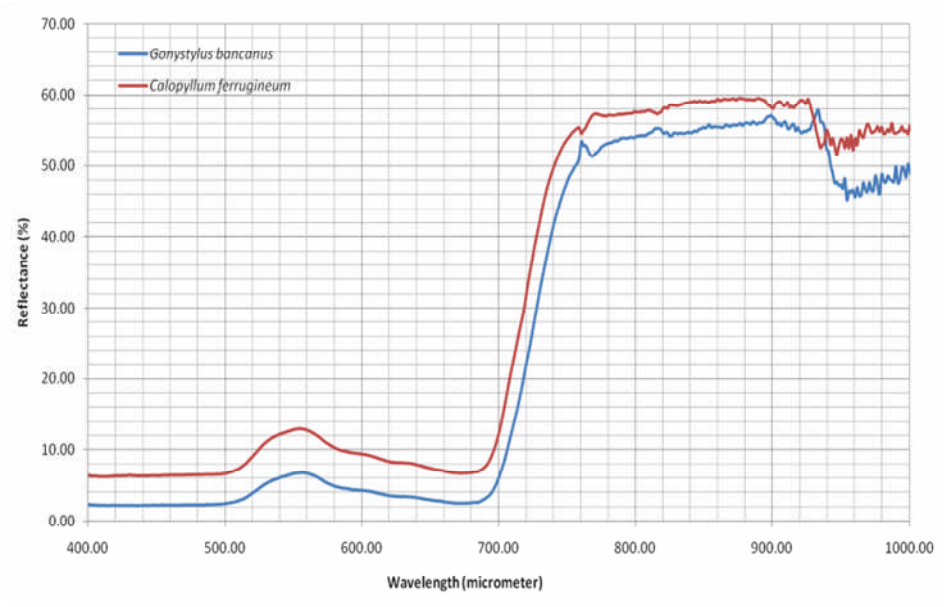

Figure 17 Spectral signatures of ramin (*Gonystylus bancanus*) and bintangor (*Calopyllum ferrugineum*)

To make sure that the sample of ramin trees that was selected in hyperspectral imagery was a true ramin tree, the data were correlated with the field survey data measurement. The result shows a good correlation (with R^2 of 0.991) between ramin spectral signature measured using spectroradiometer and the selected ramin spectral signature from hyperspectral data as shown in Figure 18.

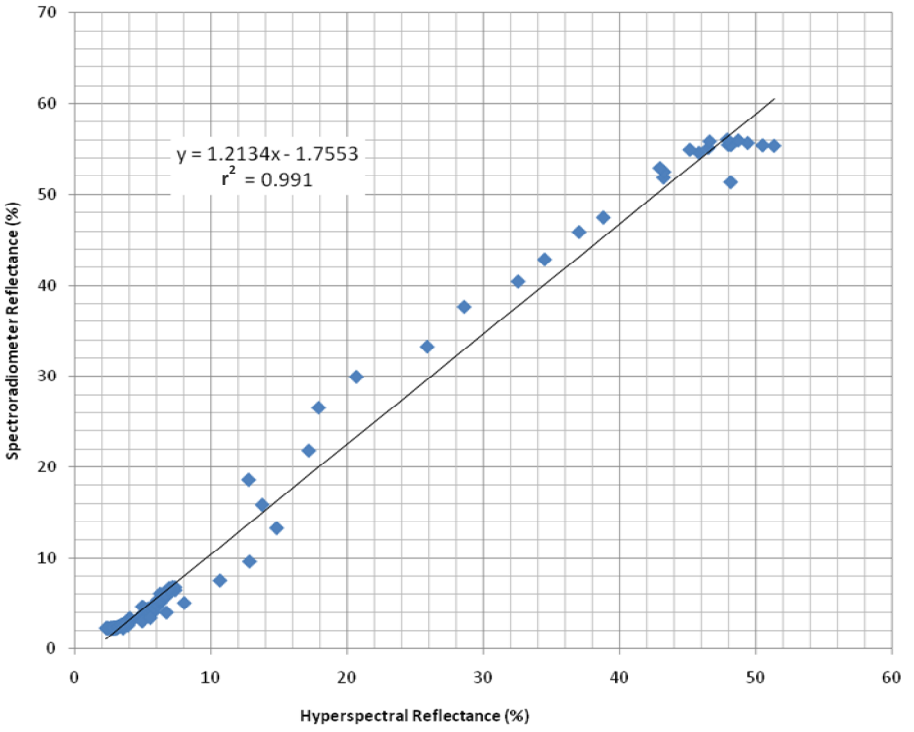

Figure 18 Correlation between hyperspectral and spectroradiometer reflectances of ramin

Tree Inventory

The purpose of the inventory was to collect training data for the hyperspectral image classification and data accuracy assessment of the classification output. The fieldwork was conducted in Compartment 77, Pekan Forest Reserve, Pahang. During an extensive field survey, several hundreds of ramin trees were enumerated and their geographic locations were recorded based on the established DGPS datum in the study area. Table 5 shows an example of tree inventory worksheet that was used to record parameters measured in the study.

Table 5 Example of tree inventory worksheet

Start point	To/Tree ID	Azimuth (Degree)	Distance (m)	DBH (cm)	1st branch (m)	Total height (m)	Canopy (m)	Note
CP1	CP2	71.9	16.10					
CP2	R1	64.4	13.60	40.00	26.5	32.00	8x4	
	R2	76.4	11.80	29.50	14.2	19.30	3x4	
	CP3	250.9	16.50					
CP3	CP4	265.5	17.30					
CP4	R3	254.1	16.80	50.00	22.0	32.80	6x5	
	CP5	258.5	16.20					
CP5	R4	292.1	12.10	46.90	28.6	45.40	4x5	
	CP6	289.6	11.50					
CP6	R5	355.3	12.80	57.10	35.8	46.60	5x4	
	CP7	234.4	24.70					
CP7	CP8	357.4	5.00					
CP8	R6	66.2	23.50	61.50	25.4	44.40	6x6	
	CP9	281.7	17.80					
CP9	R7	279.6	11.70	46.50	28.6	47.30	5x4	
	CP10	276.1	11.40					
CP10	R8	250.3	14.80	54.10	19.6	29.20	4x5	
	R9	294.8	16.10	37.50	19.3	26.50	6x5	
	R10	265.4	26.70	58.80	22.2	32.90	7x7	
CP8	CP11	356.5	13.70					
	R11	337.1	11.00	50.00	23.3	44.70	6x5	
	CP12	264.7	19.40					
CP12	R12	269.3	18.40	56.10	19.0	38.70	6x4	
	CP13	356.1	11.20					
CP13	R13	301.5	13.90	36.50	23.5	31.80	5x6	

In this project, ramin tree inventory data were collected from field survey in the test site as described in Section Tree Inventory (Chapter 3). A total of 670 ramin trees were enumerated in the study area. This included 491 trees from 25 ha of virgin PSF and 179 trees from the 30 ha of logged over PSF. The average densities of ramin trees in the virgin and logged-over PSF plots were 19.54 and 5.97 trees/ha respectively. The mean height of the ramin trees was about 34.7 m, while the dbh ranged from 21.6 to 83.5 cm. All parameters and data collected from the field inventory were kept in a Geographic Information System (GIS) database (Figure 19).

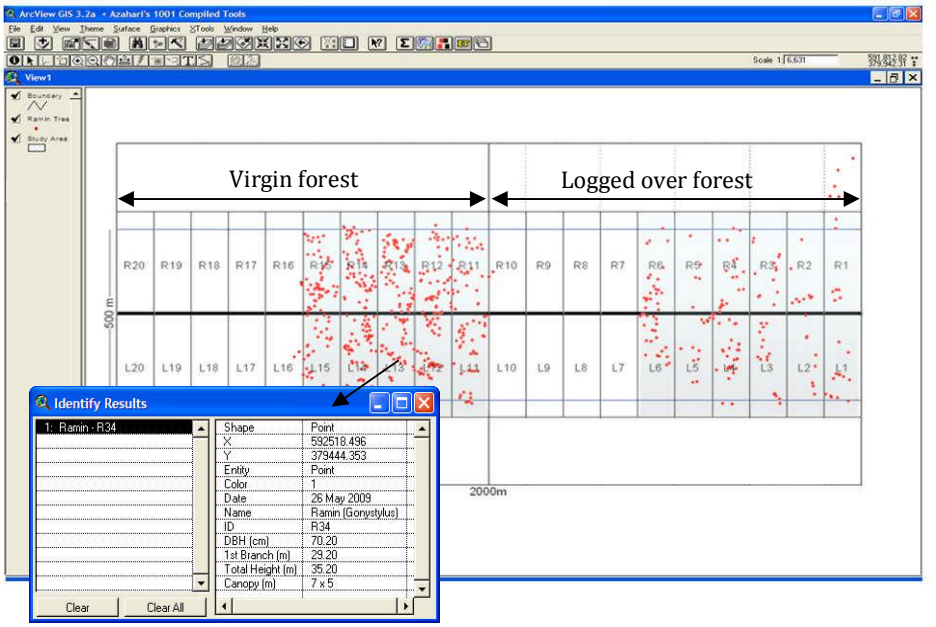

Figure 19 Ramin GIS database

Ramin Classification Using Hyperspectral Data

Having general information on the subject to be classified in the remote sensing image will help to increase the accuracy of the data to be classified. In this study the classification of ramin in the hyperspectral data was done with the help of information on ramin position collected from the field survey. The selected ramin tree that has been identified was used as a sample to generate ramin spectral signature in the SAM classification technique and consequently to identify all pixels with similar characteristics (Figure 20). Finally the information was used to map the ramin distribution in the entire image.

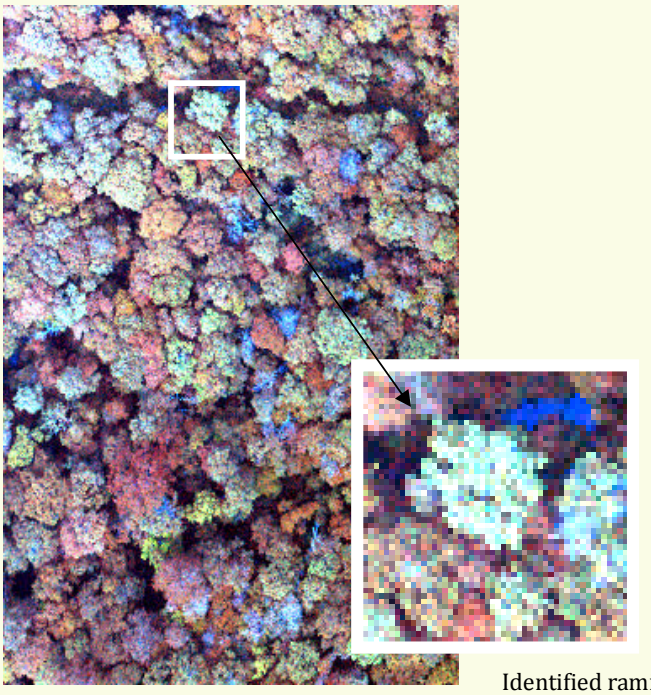

Figure 20 Example of identified ramin tree selected as sample point

Vegetation classification in the hyperspectral image can be regarded as a technique of object identification and mapping. The unknown pixels in the image are identified as among several vegetation types whose reference spectra are derived from the hyperspectral imagery by means of Regions of Interest (ROI). Ideally, the reflectance spectra of each vegetation type should not vary, but in reality it does, due to a number of factors, including the phenological stage, weather conditions, soil conditions, shadows, and Bidirectional Reflectance Distribution Function (BRDF) effects. One of the most frequently applied strategies for object mapping is the use of similarity measures. This study makes use of a deterministic similarity measure to compare an unknown pixel spectrum with a library of reference spectra using SAM.

The end member spectra of ramin used by the SAM technique in this study were obtained from the selected ramin signature sample from HySpex images that have been identified from the field survey. Strong spectral differences between ramin and other tree species classes are the main factor to discriminate this species in mixed peat swamp forest using the SAM technique. In this study, each of the selected ramin signatures that have been identified in hyperspectral data was treated as an individual

end member in the SAM classification technique. In other words, they contain only one representative spectrum per target. This is because the ramin trees in the area were showing different blooming stages during the data acquisition (Figure 21).

The different blooming stages of ramin in the study area lead to the variation of reflectance magnitude of some ramin trees in the hyperspectral data. Instinctively this could explain some of the difficulties in distinguishing ramin in the peat swamp forest in this study.

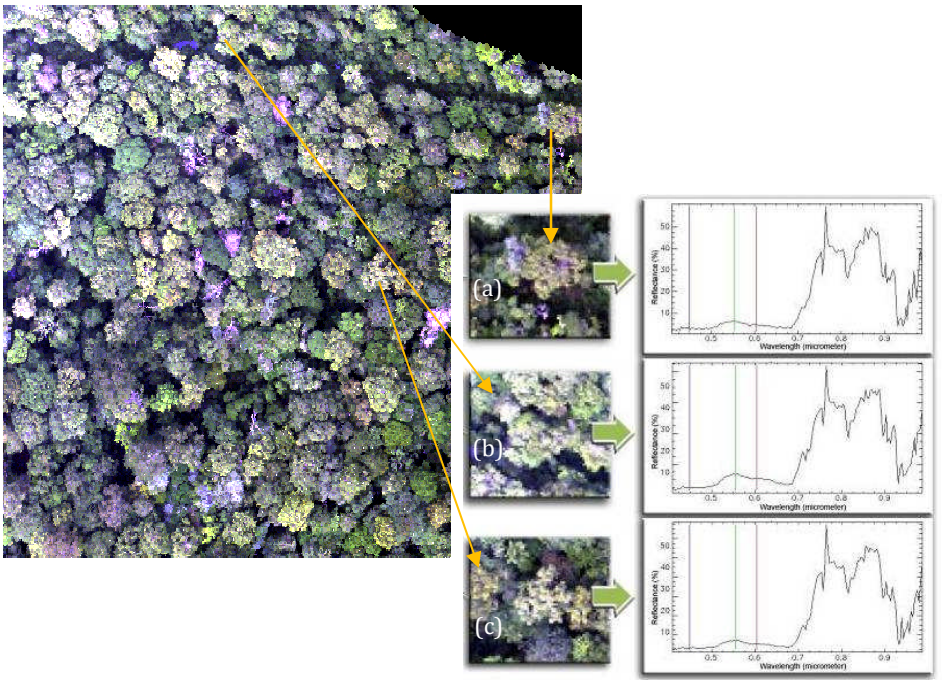

Figure 21 Signatures of different ramin blooming stages: (a) blooming, (b) semi blooming and (c) non-blooming

After separation of the spectral bands that are dominated by noise using MNF transformation, the standard SAM classification was performed on the hyperspectral image. To clean up the initial classification result, a standard majority 3x3 filter was applied. This filter uses a 3x3 pixels kernel and replaces the center pixel in the kernel with the class value that the majority of the pixels in the kernel have. Figure 22 shows the result of ramin tree classification after post-classification clean-up by a majority 3x3 filter.

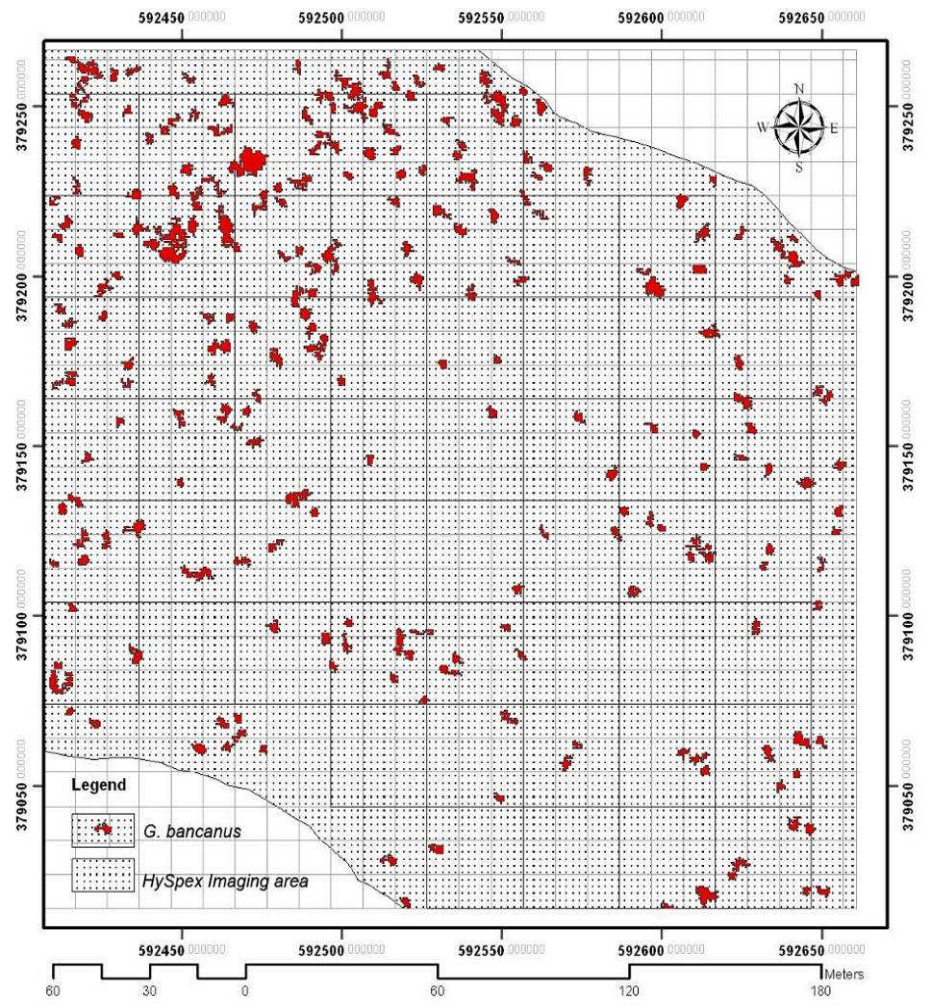

Figure 22 Ramin classification using hyperspectral data

Validation and Verification

In order to validate the results, 37 systematic plots within the study area were established. An absolute accuracy was calculated for the resulted ramin tree distributions from hyperspectral data. Absolute accuracy is a measure of the error between a derived/predicted ramin tree from airborne hyperspectral image and the actual ramin tree measured on the ground. In this study, absolute accuracy (as shown in Table 6) is expressed as the vertical root mean square error (RMSE). It was found that the distribution of ramin within the study area was about 21 trees existing in 1 ha area, with an accuracy of 86% or ± 4 trees ha^{-1}.

Table 6 Accuracy of the predicted ramin trees

Plot number	Number of trees(ramin)		Magnitude of errors	Mean square errors
	Predicted (b)	Measured (b')	(b - b')	$((b - b')-\mu)^2$
1-3	0	0	0	0.02
1-4	1	1	0	0.02
1-5	1	3	-2	3.46
1-6	1	1	0	0.02
2-0	2	1	1	1.30
2-1	2	2	0	0.02
2-2	2	8	-6	34.35
2-3	2	4	-2	3.46
2-4	2	1	1	1.30
2-5	1	0	1	1.30
2-6	0	0	0	0.02
3-1	1	3	-2	3.46
3-2	2	2	0	0.02
3-3	0	0	0	0.02
3-4	1	1	0	0.02
3-5	1	0	1	1.30
3-6	4	4	0	0.02
4-0	1	4	-3	8.19
4-1	2	0	2	4.57
4-2	2	0	2	4.57
4-3	0	0	0	0.02
4-4	1	4	-3	8.19
4-5	2	1	1	1.30
4-6	0	1	-1	0.74
5-0	3	3	0	0.02
5-1	1	0	1	1.30
5-2	5	2	3	9.85
5-4	0	6	-6	34.35
5-5	0	0	0	0.02
6-0	3	5	-2	3.46
6-1	6	0	6	37.69
6-3	4	2	2	4.57
6-5	0	2	-2	3.46
6-6	4	5	-1	0.74
7-0	4	4	0	0.02
7-2	6	2	4	17.13
			μ = 0.14	**RMSE = ± 4.1 tree/ha**

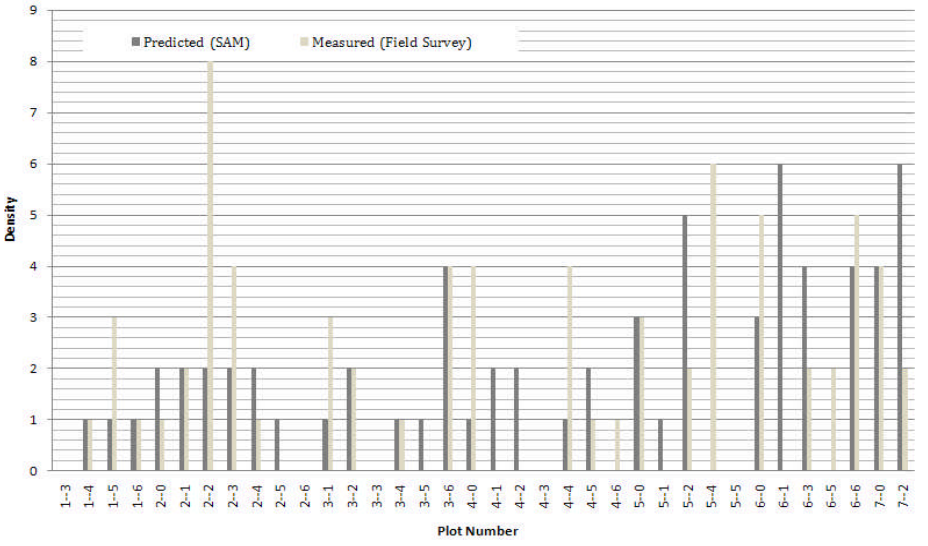

Figure 23 Comparison between field survey mapping and hyperspectral mapping

Ramin Tree Volume Estimation

Volume estimation can be made from the information derived from hyperspectral image analysis as a value-added product of hyperspectral data. In this study, the estimation of ramin tree volume has been done by delineating the individual tree crown areas from hyperspectral data. A single crown or canopy is treated as a single tree. The volume was estimated from the correlation between tree dbh and tree crown size. Volume of each tree was calculated using the equation from Ismail (2009).

$$\text{Ln}(V) = -7.2213 + 2.1057 \times \text{Ln}(\text{dbh (cm)}) \quad \text{- Equation 1}$$

where,

V = volume (m^3)
dbh = Diameter at breast height

A simple linear regression model for predicting volume from the crown area was developed using the 20 samples of tree crown with dbh ranging 25 - 64 cm. The value for r^2 was 0.728 for this fit of the model (Figure 24). The equation developed in this study was V = 0.0311 (crown size) - 0.0435, where it provided a means for predicting volume from the crown size measurement using the hyperspectral images. A comparison of tree volume estimation between volume measured using equation developed

by Ismail (2009) and volume estimated using hyperspectral images is presented in Table 7. The high accuracy of the volume estimated using hyperspectral images indicates the usefulness of the data for ramin volume estimation in the natural forest environment.

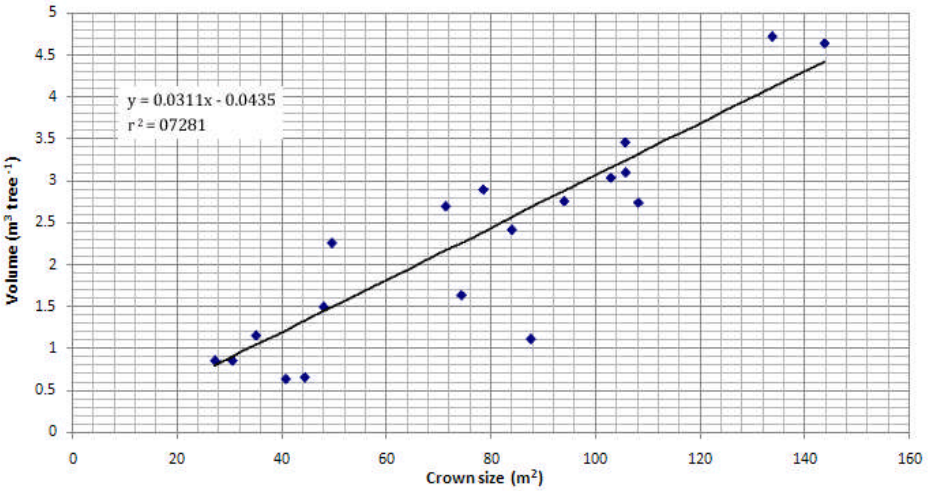

Figure 24 Correlation between crown size and stem volume

Table 7 Accuracy of tree volume estimation

DBH (cm)	Crown Area (m^2)	Measured Volume (using Equation 1) (m^3 $tree^{-1}$)	Estimated Volume (m^3 $tree^{-1}$)
52.3	102.91	3.04	3.16
64.0	143.48	4.65	4.42
64.5	133.58	4.72	4.11
32.6	87.40	1.12	2.67
33.2	35.14	1.17	1.05
25.0	40.93	0.64	1.23
49.5	71.15	2.7	2.17
49.8	107.9	2.74	3.31
55.6	105.4	3.45	3.24
39.1	74.31	1.65	2.27
50.0	93.94	2.76	2.88
47.0	84.02	2.43	2.57
37.5	48.03	1.51	1.45
28.6	30.60	0.85	0.91
51.2	78.43	2.90	2.40
52.8	105.4	3.10	3.24
28.7	27.35	0.86	0.81
			Standard error: ±1.6 m^3 $tree^{-1}$
			Accuracy: 97.3%

CHAPTER 5
OVERVIEW AND RECOMMENDATIONS

Problems and limitations

Various studies in temperate conifer and mixed deciduous forests have demonstrated accurate empirical estimates of canopy chemistry from airborne hyperspectral technology. However, this application is relatively new in tropical forests, thus may introduce new challenges, i.e. weather conditions and varying forest composition.

The airborne hyperspectral technology is a relatively new technology in forestry and only few companies offer such services in Malaysia. As such only limited options are available in choosing a suitable and reliable company to acquire hyperspectral data. In addition there is a standard procurement process to be followed by government agencies, and this needs to be taken into consideration at the early stage of project planning in order to avoid unnecessary data acquisition delay. The acquisition of the airborne hyperspectral data also requires approval from the Department of Civil Aviation (DCA), Malaysia because the installation of hyperspectral system equipment needs some modification to the aircraft which will further prolongs the process of getting the hyperspectral data. Together with unpredictable weather condition, all these factors may contribute to the delay in getting hyperspectral data in a developing tropical country like Malaysia.

During the acquisition of airborne hyperspectral data in the study area, ramin trees were in the floral phase. In the perspective of ecology, this tree blooming phase is very important. However, this situation caused difficulty in processing the hyperspectral data. As such for better tree species differentiation in the hyperspectral images, proper data acquisition timing is important and whenever possible try to avoid the flower blooming as well as fruiting seasons as to avoid unnecessary spectra signature interferences caused by the flowers and fruits of the trees.

This study shows that the hyperspectral remote sensing technique is a potential tool to extract information from a forest with fairly homogenous features such as peat swamp forest. With the right approach and processing and analysis procedures, variations within peat swamp can be discriminated and classified accordingly. These variations may reflect the biophysical properties of the peat swamp such as forest composition, tree

density as well as vegetation status. This study also helps in forest management and monitoring.

Conclusion

From the classification of HySpex hyperspectral image in the study area, it was found that the ability to discriminate ramin as an individual canopy tree from peat swamp forest was high. Strong spectral differences between ramin and the other tree species are the main factor to discriminate this species in mixed peat swamp forest using the SAM technique. A spectral library of the ramin trees has been developed and can be used as reference spectral library for future research projects. In this study, the ramin spectral signature has been developed using 160 of HySpex hyperspectral band. By using this spectral signature, ramin trees can be identified faster using HySpex hyperspectral data with acceptable mapping accuracy.

It was noted in the field that a large proportion of the tree crowns appearing to be single individual stands were in fact a combinations of mixed species in HySpex image. Instinctively this could explain some of the difficulties in distinguishing ramin species in the peat swamp forest. One of the more interesting results arising from this study is the effectiveness of species discrimination of individual ramin using only a few spectral bands of airborne HySpex hyperspectral data. It was found that the distribution of ramin within the study area was about 21 trees in 1 ha area, with an accuracy of 86% or ± 4 tree ha^{-1}. This study has demonstrated the Hyspex data can be used to classify an individual species as well as distinguish ramin tree crowns in mixed peat swamp forest. The discrimination of ramin using the SAM technique was robust with consistently high classification accuracies. The availability of accurate information on ramin population from this study can be used to assist in designing rehabilitation and conservation programme in order to conserve and sustainably manage this species. By lowering costs and increasing availability, such remote sensing technology could become operational for large-scale forest classification and mapping projects.

To further increase the accuracy, some actions can be taken. Firstly, the improvement of geometric accuracy of ramin sample from field survey activity. Because of wrongly selected ground data, pixels result in bad classification performance. The area of interest (AOI) for development of spectral signature need to be manually selected to make sure the selection is correct compared with ground survey data. There are three main factors determining the quality of ground survey data. The first is complexity of the classes and the landscape. The second is the amount of survey data

that are taken. The third is the amount of errors made when collecting the ground survey data.

Secondly, using Individual Tree Crown delineation could be another method to improve classification results. This approach delineates individual trees from aerial or satellite images and classifies the tree species. The Individual Tree Crown functions best performs on not too dense forest, which means no overlapping of crowns. However, the tree crowns should be large and dense enough to be detected, but this is mainly dependent on the image characteristics. On the other hand, LiDAR (Light Detection and Ranging) data and optical images may form a powerful combination of remote sensing techniques which may improve classification results. Optical images are best for classifying tree species and vegetation health, while LiDAR is best for measuring heights and densities. These two sensor types complement each other and could reduce the classification errors encountered in this study: the confusion of ground vegetation, bushes and mixed tree crowns. Incorporating height classes information captured from LiDAR data would reduce these problems. A future study focusing on this particular aspect is recommended.

REFERENCES

ABDUL RAHIM, N., EFRANSJAH, KHALI AZIZ, H., & SHAHARUDDIN, M.I. 2007. Intergrated Management Plan of the South East Pahang Peat Swamp Forest. Peat Swamp Forest Project, UNDP/GEF funded, in collaboration with the Pahang Forestry Department. 232 pp.

BUCKINGHAM, R., STAENZ, K. & HOLLINGER, A. 2002. Review of Canadian airborne and space activities in hyperspectral remote sensing. Canadian Aeronautics and Space Journal. Vol. 48.

DANSON, F. M. 1995. Development in the remote sensing of forest canopy structure. Advance in Environmental Remote Sensing : 53-69.

ISMAIL, P., ABD RAHMAN, K., WAN MOHD SHUKRI, W.A., SAMSUDIN, M. & HARFENDY, O. 2010. Development of local volume table (LVT) for peat swamp in Pekan Forest Reserve, Pahang with special reference to *Gonystylus bancanus* (ramin melawis). Paper presented at MAJURUS, 21/9/10. 14pp.

ITTO. 2007. ITTO Expert Meeting on the Effective Implementation of Inclusion of Ramin (*Gonystylus* spp.) in Appendix II of CITES – Report of the Expert Meeting, 16-19 May 2006. Aminah, H., Chen, H.K., Chua, L.S.L. & Khoo, K.C (Eds.), Kuala Lumpur, Malaysia. 176 pp.

KHALI AZIZ, H., ISMAIL, P., ANI S., MOHD AZAHARI, F., HARRY, Y., & IHSAN SABRI, K. 2010. Gonystylus bancanus – Jewel of the Peat Swamp Forest. FRIM special publication. 84 pp.

KHALI AZIZ, H., ISMAIL, P., ABD RAHMAN, K., CHE HASHIM, H., GRIPPIN, A. & NIZAM, M.S. 2009. Stand characteristics of one hectare peat swamp forest ecological plot in Pahang, Malaysia. Journal of Tropical Life Sciences Research, USM 20(2): 23-35.

MC & I. 2002. The Malaysian Criteria and Indicators for Forest Management Certification, 2002. Forestry Department Peninsular Malaysia. Unpublished report. 55 pp.

SHAFRI, H.Z.M., AFFENDI S. & SHATTRI, M. 2007. The performance of maximum likelihood, spectral angle mapper, neural network and decision tree classifiers in hyperspectral image analysis. Journal of Computer Science 3 (6): 419-423.

APPENDIX 1 Ramin (*Gonystylus bancanus*)

APPENDIX 2 Nature of peat swamp forest in Pekan Forest Reserve

APPENDIX 3 Ramin distribution map using hyperspectral data

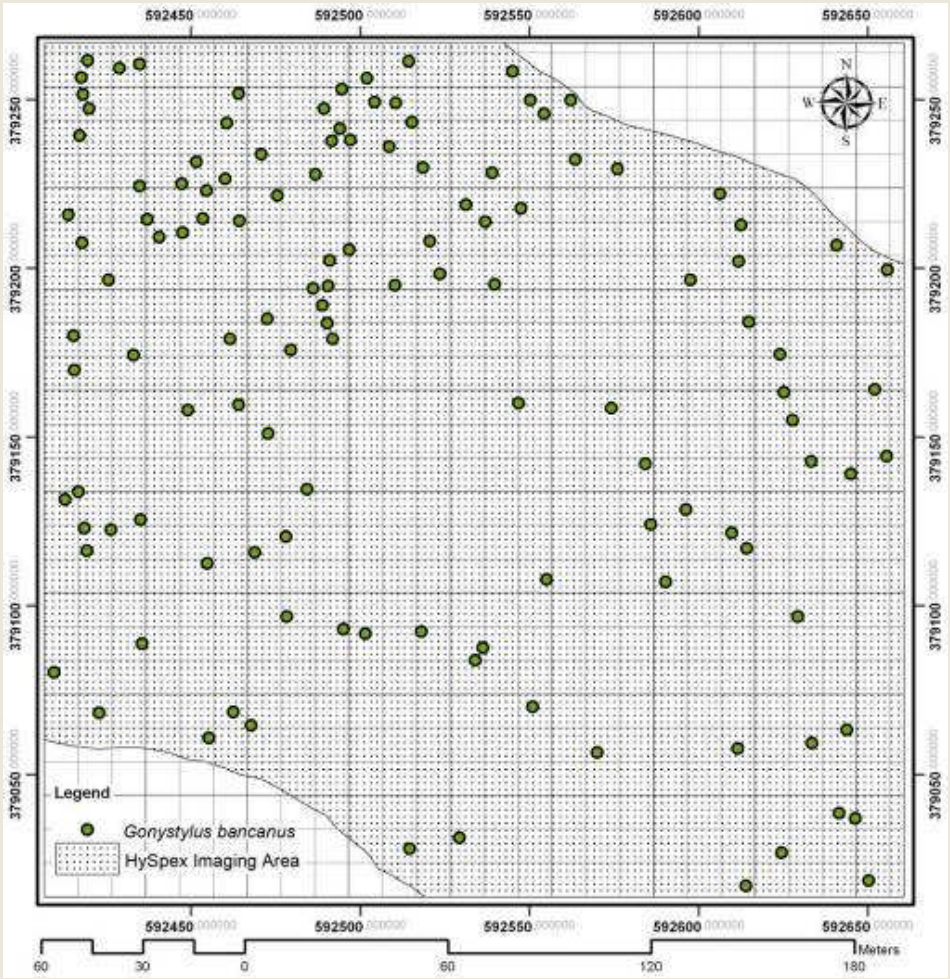

APPENDIX 4 Crown delineation and sampling points for stem volume estimation

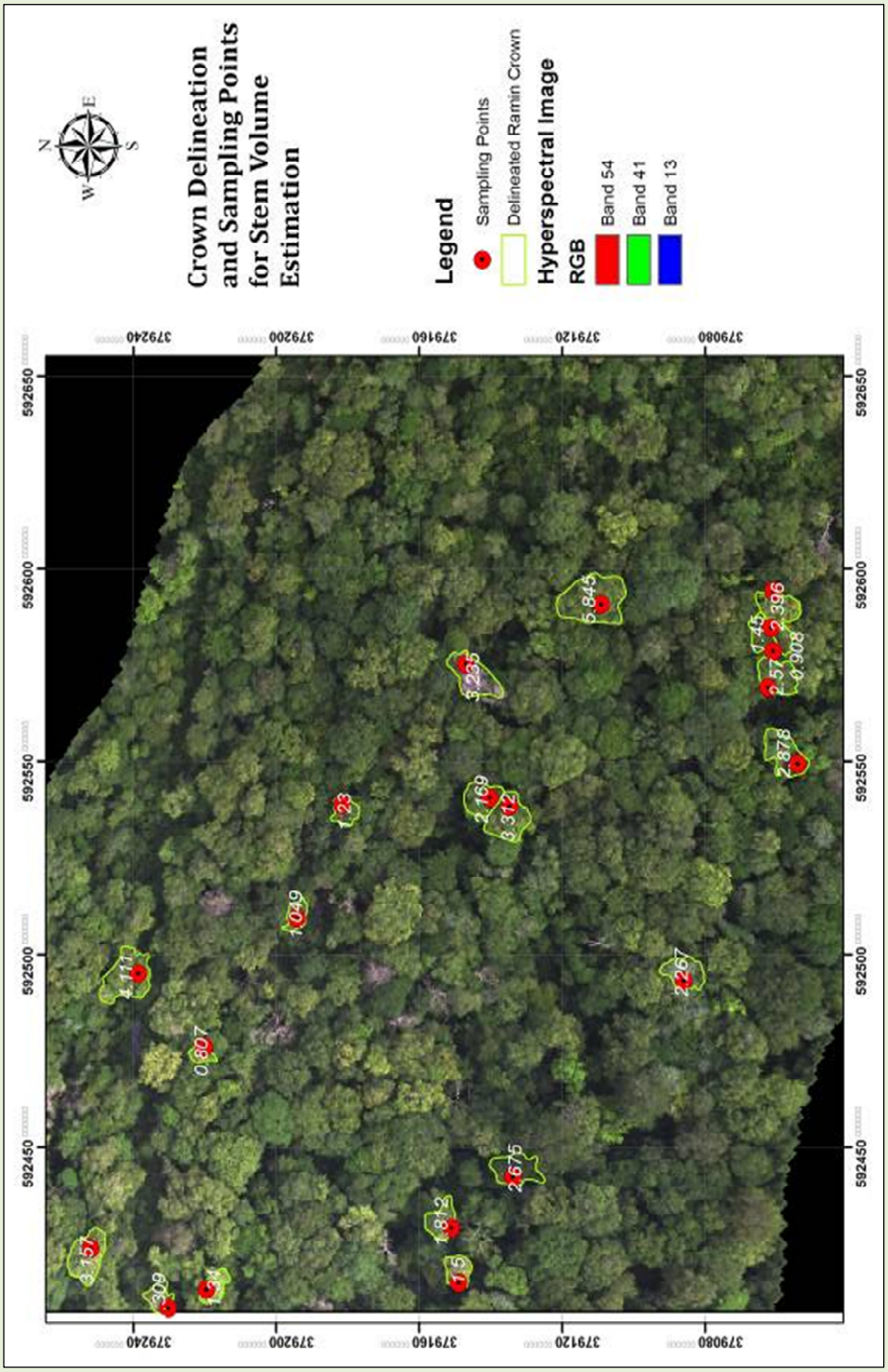

APPENDIX 5 Ramin spectral signature (reflectance) of hyperspectral and spectroradiometer data

No.	Wavelength (µm)	Reflectance (%)	
		Hyperspectral	Spectroradiometer
1	0.4085	2.41	2.23
2	0.4121	2.34	2.25
3	0.4157	2.51	2.22
4	0.4194	2.65	2.23
5	0.423	2.79	2.22
6	0.4266	2.44	2.24
7	0.4302	3.58	2.23
8	0.4339	2.90	2.20
9	0.4375	3.07	2.23
10	0.4411	2.97	2.23
11	0.4447	2.84	2.23
12	0.4484	3.14	2.27
13	0.452	2.81	2.24
14	0.4556	3.09	2.27
15	0.4593	3.02	2.28
16	0.4629	2.96	2.28
17	0.4665	2.98	2.28
18	0.4701	3.13	2.29
19	0.4738	3.04	2.29
20	0.4774	3.17	2.30
21	0.481	2.69	2.30
22	0.4846	2.86	2.29
23	0.4883	3.27	2.37
24	0.4919	3.20	2.36
25	0.4955	3.21	2.38
26	0.4991	3.30	2.45
27	0.5028	3.58	2.54
28	0.5064	3.62	2.66
29	0.51	4.11	2.91
30	0.5137	4.06	3.15
31	0.5173	5.11	3.52
32	0.5209	5.79	3.93
33	0.5245	6.08	4.60
34	0.5282	6.31	5.05
35	0.5318	6.47	5.42

36	0.5354	6.73	5.71
37	0.539	6.69	6.05
38	0.5427	7.00	6.23
39	0.5463	7.40	6.43
40	0.5499	7.27	6.61
41	0.5535	7.39	6.76
42	0.5572	7.20	6.78
43	0.5608	6.96	6.68
44	0.5644	6.89	6.49
45	0.5681	6.30	6.04
46	0.5717	6.45	5.67
47	0.5753	6.09	5.32
48	0.5789	6.05	5.04
49	0.5826	5.75	4.74
50	0.5862	4.99	4.61
51	0.5898	5.06	4.54
52	0.5934	5.41	4.41
53	0.5971	5.24	4.35
54	0.6007	5.85	4.31
55	0.6043	5.47	4.23
56	0.6079	5.52	4.12
57	0.6116	5.18	3.92
58	0.6152	5.25	3.77
59	0.6188	5.01	3.64
60	0.6225	5.19	3.51
61	0.6261	4.84	3.48
62	0.6297	5.13	3.45
63	0.6333	4.91	3.44
64	0.637	4.76	3.38
65	0.6406	4.08	3.30
66	0.6442	3.98	3.18
67	0.6478	3.92	3.03
68	0.6515	3.81	2.94
69	0.6551	3.92	2.86
70	0.6587	3.89	2.80
71	0.6624	3.76	2.70
72	0.666	3.50	2.58
73	0.6696	3.50	2.53
74	0.6732	3.56	2.52
75	0.6769	3.94	2.54

76	0.6805	3.47	2.60
77	0.6841	3.66	2.63
78	0.6877	4.99	2.99
79	0.6914	5.58	3.36
80	0.695	6.76	3.95
81	0.6986	8.07	5.01
82	0.7022	10.69	7.50
83	0.7059	12.86	9.59
84	0.7095	14.85	13.29
85	0.7131	13.79	15.82
86	0.7168	12.80	18.57
87	0.7204	17.21	21.81
88	0.724	17.93	26.55
89	0.7276	20.70	29.94
90	0.7313	25.90	33.24
91	0.7349	28.62	37.64
92	0.7385	32.57	40.43
93	0.7421	34.52	42.89
94	0.7458	37.05	45.89
95	0.7494	38.83	47.47
96	0.7675	48.17	51.34
97	0.7711	43.24	51.83
98	0.7748	43.28	52.49
99	0.7784	42.98	52.93
100	0.8401	45.84	54.61
101	0.8437	45.18	54.94
102	0.8473	46.54	55.15
103	0.8546	51.36	55.38
104	0.8582	48.00	55.49
105	0.8618	48.19	55.45
106	0.8654	50.52	55.43
107	0.8691	48.18	55.56
108	0.8727	49.42	55.68
109	0.88	48.73	55.97
110	0.8836	46.63	55.86
111	0.8872	47.92	56.07

High Resolution Airborne Hyperspectral Data

for Mapping of Ramin Distribution in Peat Swamp Forest

This book focuses on the analysis of airborne hyperspectral data to discriminate individual *Gonystylus bancanus* trees in the peat swamp forest at Pekan Forest Reserve, Pahang. The book, as far as possible, provides information on the *G. bancanus* distribution pattern in the study area and also the estimation of volume for each of the individual trees.

The book is divided into five chapters. The first provides an insight into the need for the study. Chapter 2 is a brief explanation about the hyperspectral system, data acquisition technique and spectral signature data measurement. Chapter 3 of the book highlights the methodologies used and presents the data. Chapter 4 focuses on the data analysis and interpretation of the results. Chapter 5 the final chapter, concludes the book and provides some recommendations for future studies.